ACS OMEGA

Open Access

This article is licensed under CC-BY-NC-ND 4.0

http://pubs.acs.org/journal/acsodf

Article

Stoichiometric Study on Ion Composition of a Precursor in Chemical Bottom-Up Synthesis for Peroxo-Titanate

Do Hyung Han, Hyunsu Park, Tomoyo Goto, Yeongjun Seo, Yoshifumi Kondo, Sunghun Cho, and Tohru Sekino*

Cite This: *ACS Omega* 2024, 9, 33293−33300

Read Online

ACCESS | Metrics & More | Article Recommendations | Supporting Information

ABSTRACT: Layered alkali titanates of the lepidocrocite type are gaining enormous interest in various fields owing to their unique properties. These materials are mainly synthesized through a hydrothermal alkali treatment. However, this method uses a highly concentrated alkali solution, which has high environmental impacts and is therefore unsuitable for mass synthesis. Herein, we propose an efficient method for the large-scale synthesis of layered sodium titanate structures ($Na_{2-x}H_xTi_2O_5$) using a recently reported bottom-up chemical process. The effects of the Na:Ti molar ratio in the peroxo-titanium complex ion precursor on the products are investigated through stoichiometric calculations for a molar ratio range of 10:1−1:1. The optimal ratio for the complete ionization of TiH_2 (which is the starting material) to form the peroxo-titanium complex ion is found to be 1.1:1. The amount of alkali raw material required is 99.6% lower than that required in the traditional hydrothermal method. The crystal structures and morphologies of the samples are almost identical regardless of the Na:Ti molar ratio. The precursor-derived peroxo bonds narrow the energy band gaps of the layered titanates even when the amount of titanium ions dissolved in the precursor increases. The proposed method is not only an efficient synthetic route for mass production but also has potential applications in the development of photofunctional materials.

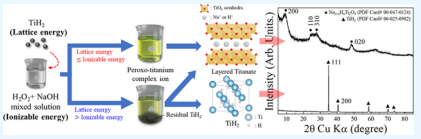

1. INTRODUCTION

Lepidocrocite-type alkali titanate has a layered structure composed of TiO_6 octahedra sharing edges and corners.[1,2] The monovalent alkali metal ion is exchangeable and positioned in the interlayer of the crystal ($A_2Ti_nO_{2n+1}$, where A can be Li^+, Na^+, or K^+, etc.).[2−4] Unlike commercial titanium dioxide (TiO_2) structures such as anatase, rutile, and brookite, this layered titanate has an anisotropic crystal structure[5,6] and can grow into a low-dimensional nanostructured material during crystal growth.[7] Because low-dimensional nanostructures have wide specific surface areas[8,9] and fast electron-transport capabilities,[10] researchers have attempted to apply them in environmental purification and eco-friendly energy generation as photocatalysts,[11] solar cells,[12] and in photoelectrochemical water splitting.[13] Alkali treatment has been used to synthesize layered alkali titanate crystals with low-dimensional nanostructures.[14,15] Traditionally, TiO_2 nanoparticles are treated with an alkaline NaOH solution. However, as TiO_2 is composed of stable Ti−O bonds with quite high bonding energies of 672.4 ± 9.2 kJ/mol,[16] a highly concentrated alkaline solution is required for producing a sufficient chemical change in TiO_2. In general, to synthesize layered sodium titanate ($Na_2Ti_2O_5$) using 1 g of TiO_2 via the hydrothermal method, 20−200 mL of NaOH solution of 10−15 mol/L concentration is required.[17] In this process, the surface of the TiO_2 crystal is exfoliated to a few layers because its Ti−O bonds are broken by the hydroxyl ions, and sodium ions are newly bonded in the interlayers to form a layered sodium titanate crystal. This layered sodium titanate crystal is reported to possess a nanosheet morphology and tends to scroll during the washing process, resulting in a nanotube morphology.[18] However, the hydrothermal method uses large amounts of alkali raw materials that have high environmental impacts and also pose a high risk to laboratory work.[18,19]

Recently, our research group reported a method for the synthesis of peroxy group (−O−O−)-modified titanate nanotubes (hereafter denoted as PTNTs), which had unique visible light responsive photocatalytic properties, via a bottom−up chemical process using an ionic precursor.[11,20,21] The peroxo-titanium complex (PTC) ion solution ($Ti[(OH)_3O_2]^-$) used as a precursor was prepared by ionizing TiH_2 in a mixed solution of H_2O_2 and NaOH, in which the NaOH concentration was significantly lower (1.5 mol/L) than that of the traditional hydrothermal method (10 mol/L).[11] Furthermore, peroxo-titanium complex ion was directly transformed into a sodium titanate crystal structure at 100 °C under atmospheric pressure[20] because TiH_2 contained Ti−H bonds with weaker bonding energies (226.6 ± 10.6 kJ/mol) than the Ti−O bonds; thus, the energy required to dissolve

Received: June 11, 2024
Revised: July 9, 2024
Accepted: July 11, 2024
Published: July 22, 2024

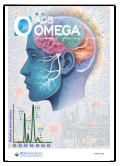

© 2024 The Authors. Published by American Chemical Society

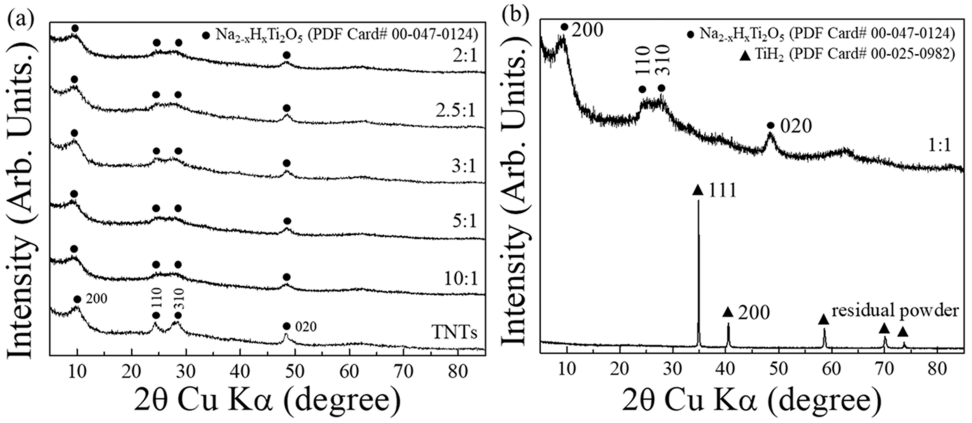

Figure 1. XRD patterns of the titanate samples of (a) 10:1, 5:1, 3:1, 2.5:1, 2:1, and TNTs, (b) 1:1 and residual powder.

and form layered sodium titanate was relatively lower.[22−24] To prepare the PTC ion precursor, a Na:Ti molar ratio of 10:1 was used in this method.[20] However, considering that the theoretical Na:Ti molar ratio in the $Na_2Ti_2O_5$ structure is 1:1, it may be possible to reduce the Na:Ti ratio in the synthesis reaction further.

As mentioned above, in this synthesis process, NaOH played two important roles: it promoted TiH_2 ionization and the formation of a titanate layer structure.[20,25] Therefore, the amounts of NaOH and TiH_2 need to be optimized to develop a synthetic method for PTNTs with a low environmental impact. In this study, to determine the optimal amount of TiH_2 for NaOH production, the effects of the Na:Ti ratio on the synthesis of $Na_2Ti_2O_5$ for large-scale production were evaluated using stoichiometric calculations. Furthermore, the crystal structure, chemical composition, morphology, surface, and optical properties of the final products (PTNTs) were examined from the perspective of TiH_2 ionization and formation of a layered structure.

2. EXPERIMENTAL SECTION

2.1. Synthesis of PTC Ion Precursor. PTC ion precursors were synthesized using the methods described in a previous study.[20] H_2O_2 (30%, FUJIFILM Wako Pure Chemical Laboratory Corporation, Osaka, Japan) solution (62.5 mL) and 10 mol/L NaOH (97%, FUJIFILM Wako Pure Chemical Laboratory Corporation, Osaka, Japan) solution (15.29 mL) were mixed to prepare a NaOH solution of concentration 1.5 mol/L and pH 10. Then, TiH_2 (>99%, Kojundo Chemical Laboratory Co., Ltd., Saitama, Japan) powder was ionized by adding 0.63, 1.25, 1.87, 2.49, 3.12, and 6.25 g to the prepared mix solution (NaOH and H_2O_2) using a magnetic stirrer under cooling at 5 °C for 24 h, in which the Na:Ti molar ratios were 10:1, 5:1, 3:1, 2.5:1, 2:1, and 1:1, respectively. The prepared PTC ion solutions were collected using a syringe filter with a pore size of 0.2 μm to remove the remaining TiH_2 and/or impurities that were not ionized. For a ratio of 1:1, a filtered powder was obtained, which was separated and analyzed.

2.2. Synthesis of Peroxy Group Modified Titanate. The prepared PTC ion solution was heated at 100 °C for 24 h with stirring at 200 rpm in a refluxing vessel under atmospheric pressure, where the solution was kept boiling during the reaction. After the reaction, the precipitates were repeatedly washed with ultrapure water and filtered by using a vacuum pump (MDA-020C, ULVAC, Inc., Kanagawa, Japan) until the ionic conductivity of the filtered solution reached approximately 5 μS/cm. After washing, the collected samples were dried using a freeze-dryer (EYELA FDU-2200, Tokyo Rikakikai Co., Ltd., Tokyo, Japan) and labeled according to the Na:Ti molar ratio. As a reference for comparison, nonmodified pristine titanate (titania nanotubes, TNTs)[14] was prepared for evaluating the crystallographic and optical characteristics. Commercial nanosized TiO_2 powder (1 g, P25, NIPPON AEROSIL Co., Ltd., Tokyo, Japan) as a precursor was mixed with 400 mL of a 10 mol/L concentrated NaOH solution and heated at 115 °C for 24 h with stirring at 200 rpm in a refluxing vessel under atmospheric pressure. To evaluate the effect of synthesis temperature, the PTC ion solution was sealed in a Teflon autoclave and heated at 115 °C for 24 h without stirring or shaking. The obtained precipitates were also washed and dried in the same manner (as described above).

2.3. Characterization. The crystal phases of the samples were characterized by X-ray diffraction (XRD; D8 ADVANCE, Bruker AXS Co. Ltd., Karlsruhe, Germany). The diffraction patterns of the structures were obtained using a Scintag diffractometer, operated in the Bragg configuration with Cu Kα radiation (λ = 1.54 Å) from 5−85° at a scanning rate of 0.02°. X-ray fluorescence (XRF; ZSX100e, RIGAKU, Tokyo, Japan) spectroscopy was used to calculate the molar ratios of Na and Ti in the samples in EZ scan mode. X-ray photoelectron spectroscopy (XPS; JPS9010MX. JEOL Ltd., Tokyo, Japan) was performed to measure the O_{1s} spectra, and the binding energy was standardized with respect to the C_{1s} energy. The chemical structures of the samples were measured using a Fourier transform infrared (FT-IR) spectrometer (FT/IR4100, JASCO, Tokyo, Japan) within the range 4000−500 cm^{-1} at a resolution of 4 cm^{-1} using the KBr pellet method in transmission mode. Ultraviolet−visible (UV−vis) spectroscopy (V-650, JASCO Corporation, Tokyo, Japan) was used to analyze the optical properties such as the reflectance and band gap energies of the samples. The morphologies of the samples were observed by field-emission scanning electron microscopy (FE-SEM; SU-9000, Hitachi High-Technologies Corporation, Tokyo, Japan) using secondary electron (SE) and scanning transmission electron (STEM) imaging modes at an acceleration voltage of 30 kV.

Stoichiometric analyses were performed to investigate the relationship between the theoretical and experimental values of the ionizable amount for mixed solution (NaOH and H_2O_2), and the maximum synthetic yields for the synthesized samples were obtained through lattice energy calculations. In general, the energy required to ionize a crystalline material is called the

https://doi.org/10.1021/acsomega.4c05470
ACS Omega 2024, 9, 33293−33300

lattice energy. The lattice energy can be calculated using the Born−Landé equation, as follows:[26]

$$U = \frac{N_A \cdot M \cdot |z^+ \cdot z^-| \cdot e^2}{4\pi \cdot \varepsilon_0 \cdot r}\left(1 - \frac{1}{n}\right) \quad (1)$$

where U is the lattice energy, N_A is the Avogadro constant, M is the Madelung constant, z^+ and z^- are the charge numbers of the cation and anion, respectively, e is the elementary charge, ε_0 is the permittivity of free space, r is the distance to the closest ion, and n is the Born exponent.

3. RESULTS AND DISCUSSION

Figure 1a shows the XRD patterns of the control TNTs and the samples with Na:Ti molar ratios of 10:1, 5:1, 3:1, 2.5:1, and 2:1. The XRD patterns of all titanate samples with molar ratios in the range of 10:1−1:1 exhibited broad peaks corresponding to the lepidocrocite-type layered titanate crystal structure assigned to $Na_{2-x}H_xTi_2O_5$ (PDF Card 00-047-0124), and there were no impurities regardless of the molar ratio. The 200, 110, 310, and 020 crystal planes of the layered titanate structure were observed with diffraction peaks (2θ) at 9.3, 24.4, 28.1, and 48.3°, respectively. In particular, the d-spacing of the 200 plane was related to the interlayer distance of the layered structure, which changed according to the type of cation or chemical bonding between the layers.[7,27] For sodium titanate ($Na_2Ti_2O_5$), the Na^+ cation present in the interlayer could be exchanged with the H^+ cation during the washing process, as indicated by the structural formula $Na_{2-x}H_xTi_2O_5$. The 200 diffraction peaks of all samples exhibited the same degree with 9.3°, which implied that Na^+ and H^+ existed in the same ratio in each sample.

The chemical compositions of all titanate samples, calculated from the Na and Ti detection results of the XRF analysis, are listed in Table 1. All samples had a chemical composition

Table 1. Content of Sodium and Chemical Composition of the Titanate Samples Calculated from XRF Results

Na:Ti (molar ratio)	content of sodium (%)	chemical composition
10:1	8.81	$Na_{0.52}H_{1.48}Ti_2O_5$
5:1	8.43	$Na_{0.49}H_{1.51}Ti_2O_5$
3:1	9.02	$Na_{0.54}H_{1.46}Ti_2O_5$
2.5:1	8.54	$Na_{0.50}H_{1.50}Ti_2O_5$
2:1	8.68	$Na_{0.51}H_{1.49}Ti_2O_5$
1:1	8.79	$Na_{0.52}H_{1.48}Ti_2O_5$
TNTs	8.32	$Na_{0.49}H_{1.51}Ti_2O_5$

similar to that of the $Na_{0.5}H_{1.5}Ti_2O_5$ structure. Because unreacted substances remained in the 1:1 molar-ratio sample in the synthesis experiment of the PTC ion precursor, the residue was separated from the solution. Figure 1b shows the XRD patterns of the titanate and filtered residual powder in the 1:1 molar-ratio sample. The residue exhibited a TiH_2 (PDF Card# 00-025-0982) crystal structure, corresponding to the region where TiH_2 was not ionized. These results suggested that a 1:1 molar ratio was insufficient for the ionization of TiH_2 in this process.

Table S1 shows the yield of the titanate sample, which was calculated based on the weight of titanate theoretically predicted from the weight of TiH_2 and the weight of the titanate synthesized experimentally. The chemical composition of the theoretically predicted titanate was $Na_{0.5}H_{1.5}Ti_2O_5$, based on the XRF analysis results (Table 1).

Figure 2 shows the relationship between the weights of the titanate samples, obtained experimentally and calculated

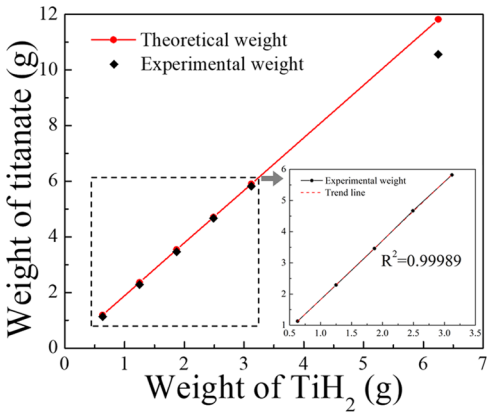

Figure 2. Weight relationship between used TiH_2 and synthesized titanate (experimental and theoretical values).

theoretically according to the weight of TiH_2 used. As shown in Table S1 and Figure 2, as the weight of TiH_2 increases, the weight of the synthesized titanate increases linearly. Furthermore, in the molar ratio range of 10:1−2:1, the trend line is fitted well with the R-squared value of 0.99989, and the yield of synthesized titanate is 94.9−99.1%. These results show that titanate is successfully and uniformly synthesized, regardless of the weight of TiH_2 in the range of 10:1−2:1. In contrast, as mentioned above, TiH_2 is not completely ionized during the ionization process in a molar ratio of 1:1. Therefore, the yield of titanate synthesized at a molar ratio of 1:1 is lower (89.3%) than that for other molar ratios. Although the theoretically required molar ratio of Na:Ti for the synthesis of the $Na_2Ti_2O_5$ structure has been estimated to be 1:1, the theoretical ratio was not actually reached in this result. Therefore, stoichiometric analysis was also performed to determine the relationship between the theoretical and experimental values and the maximum synthetic yield using the Born−Landé equation.

A schematic image of the ionization experiment using TiH_2 (1:1 molar ratio) and TiO_2 (rutile) as a control is presented in Figure 3.[28] The lattice energy of TiH_2 is calculated as 3104 kJ/

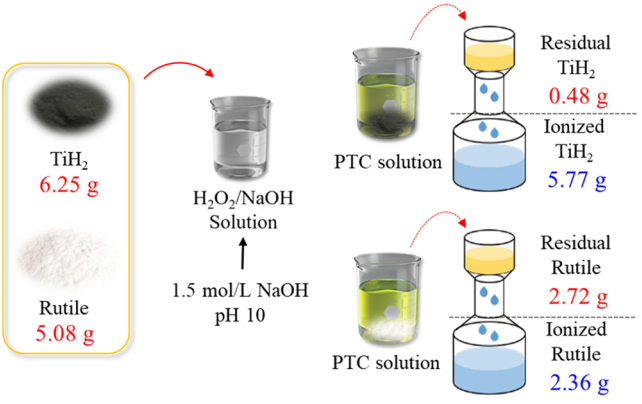

Figure 3. Schematic image of TiH_2 and TiO_2 (Rutile) ionization processes in the stoichiometric calculation.

https://doi.org/10.1021/acsomega.4c05470
ACS Omega 2024, 9, 33293−33300

mol. When ionizing 6.25 g of TiH_2 (corresponding to 1:1), 0.48 g of TiH_2 remains, while 5.77 g of TiH_2 is fully ionized. The maximum ionizable amount of TiH_2 in the mixed solution is estimated to be 5.77 g. Thus, the ionizable energy of the mixed solution is estimated to be 359 kJ, based on the relationship between the lattice energy (3104 kJ/mol) of TiH_2 and the maximum ionizable amount of TiH_2 (5.77 g). When ionizing 5.08 g of TiO_2, 2.36 g is ionized. In contrast, the lattice energy of rutile TiO_2 has been calculated to be 11 924 kJ/mol, according to eq 1. The maximum ionizable energy is calculated to be 352.5 kJ, from the amount of ionized TiO_2 (2.36 g). The calculated values for the ionization energy are similar for both TiH_2 and TiO_2, which proves the validity of this calculation approach. These stoichiometric calculations and experiments allow the prediction of the ionization properties of target materials, which depend on their lattice energies.

However, although the Na:Ti molar ratio in $Na_2Ti_2O_5$ is 1:1, this study shows that the amount of Na required for producing the final product is greater than that of Ti because of the limitation on the amount that can maximally ionize TiH_2. This is confirmed by the fact that the 0.48 g of TiH_2 remained without being ionized for the Na:Ti ratio of 1:1 as mentioned before as well as shown in Figure 3. Figure S1 shows the XRD patterns of titanate synthesized with a 1.1:1 (Na:Ti) molar ratio, which has been identified to possess a layered titanate crystal structure similar to that of the TNTs. Therefore, a 1.1:1 ratio is selected as the optimal condition in our method, and the synthesized sample is labeled "peroxo-titanate" to avoid confusing it with the other samples. In the condition of 1.1:1 (Na:Ti) molar ratio, the amount of NaOH used is reduced by 99.6%, compared to that in the traditional hydrothermal method, and 89.2%, compared to that in the initial bottom-up process.

As mentioned above, despite having the same crystal structure, there is a noticeable difference in the crystallinities of the TNTs and synthesized titanate samples, as shown in the XRD patterns in Figure 1. Because the synthesis temperature can affect the crystallinity of the materials,[29,30] the difference in crystallinity between the materials may be due to the temperature. On the other hand, pristine TNTs and titanate synthesized using the bottom-up method require 10 and 1.5 mol/L NaOH solutions, respectively. The difference in concentration causes a change in the boiling point of the mixed solution—reported to be 115 and 102 °C in the case of the 10 and 1.5 mol/L NaOH solutions, respectively,[31] due to the effect of the increase in molar boiling point. The hydrothermal method, which is used in the synthesis of pristine TNTs, uses a sealed container. Increasing the pressure inside the container allows the boiling temperature to increase; thus, this method can easily produce materials with high crystallinity. Thus, the PTC ionic precursor is treated by a hydrothermal method to attempt the synthesis at 115 °C, similar to the case of TNTs.

Figure 4 shows that the XRD pattern of peroxo-titanate synthesized at 115 °C (assigned to peroxo-titanate 115) is comparable to that of the TNTs synthesized at 115 °C and the peroxo-titanate synthesized at 100 °C. The crystallinity of each sample was evaluated by measuring the full width at half-maximum (FWHM) of the 200 plane, which is the main peak of layered titanate.

Table 2 lists the FWHM and 2θ of the 200 planes of each sample. The FWHM of TNT is 2.3, whereas that of peroxo-titanate is 2.6, with a broad peak. In contrast, the FWHM of the peroxo-titanate 115 plane is 2.3, which indicates that crystallinity can be improved by increasing the synthesis temperature. Therefore, a layered titanate structure is successfully synthesized from a PTC ion solution at a boiling point of 102 °C. Its crystallinity can be enhanced by controlling the synthetic temperature using the hydrothermal method. It is found from Table 2 that the d_{200} (interlayer lattice distance) values of peroxo-titanate and TNTs are 9.53 and 8.96 Å, respectively. As mentioned above, d_{200} of the layered structure depends on the amount and type of cations and chemical bonds between the layers. Because the type of cation is the same as that of Na^+ cations and both chemical compositions are similar, as explained in the XRF results (Table 1), the chemical bonds existing within the structure are investigated. Previously, our research group had reported the presence of a peroxy functional group (−O−O−) in the interlayer of titanate synthesized by the bottom−up method.[11] The peroxo-titanium complex ion, as the precursor, can introduce peroxo bonds into the final structure via a bottom-up crystal growth.

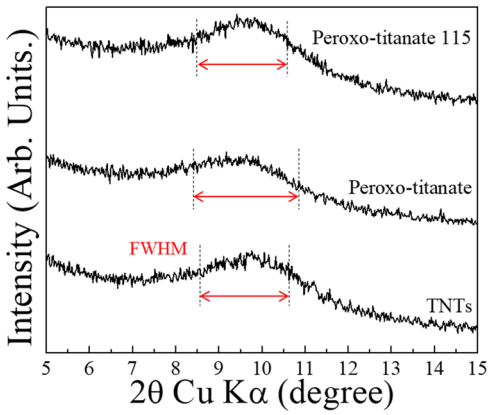

Figure 4. XRD patterns range of 5−15° and FWHM line of peroxo-titanate 115, peroxo-titanate, and TNTs.

Table 2. FWHM, 2θ, and Interlayer Distance of (200) Peak of Peroxo-Titanate 115, Peroxo-Titanate, and TNTs

sample	FWHM (deg)	2θ (deg)	d_{200} (Å)
peroxo-titanate 115	2.3	9.73	9.07
peroxo-titanate	2.6	9.27	9.53
TNTs	2.3	9.86	8.96

XPS and FT-IR analyses were conducted to detect the peroxo bonds in the samples. Figure 5a shows the XPS O 1s spectra of peroxo-titanate and TNTs. The O 1s spectrum of peroxo-titanate is separated into three peaks corresponding to Ti−O, Ti−OH, and Ti−O−O (peroxo bonding) at 530.0, 531.5, and 533.0 eV, respectively.[11,32] On the other hand, the XPS O 1s spectrum of the conventional TNTs is separated into only two peaks, corresponding to Ti−O and Ti−OH. Figure 5b shows the entire range of the FT-IR spectra of peroxo-titanate and TNTs. The peaks at 3400 and 1630 cm^{-1} are attributed to the hydroxy group (O−H) and H−O−H bonding vibrations associated with H_2O molecules, and the peak at 920 cm^{-1} corresponds to the Ti−OH bonding.[21,33,34] Furthermore, as shown in the FT-IR spectra in the range of 1200−600 cm^{-1} (Figure 5c), the transmittance intensity of the Ti−OH peak decreases in peroxo-titanate by comparing with TNT, while another peak near 880 cm^{-1} appears, which is

https://doi.org/10.1021/acsomega.4c05470
ACS Omega 2024, 9, 33293−33300

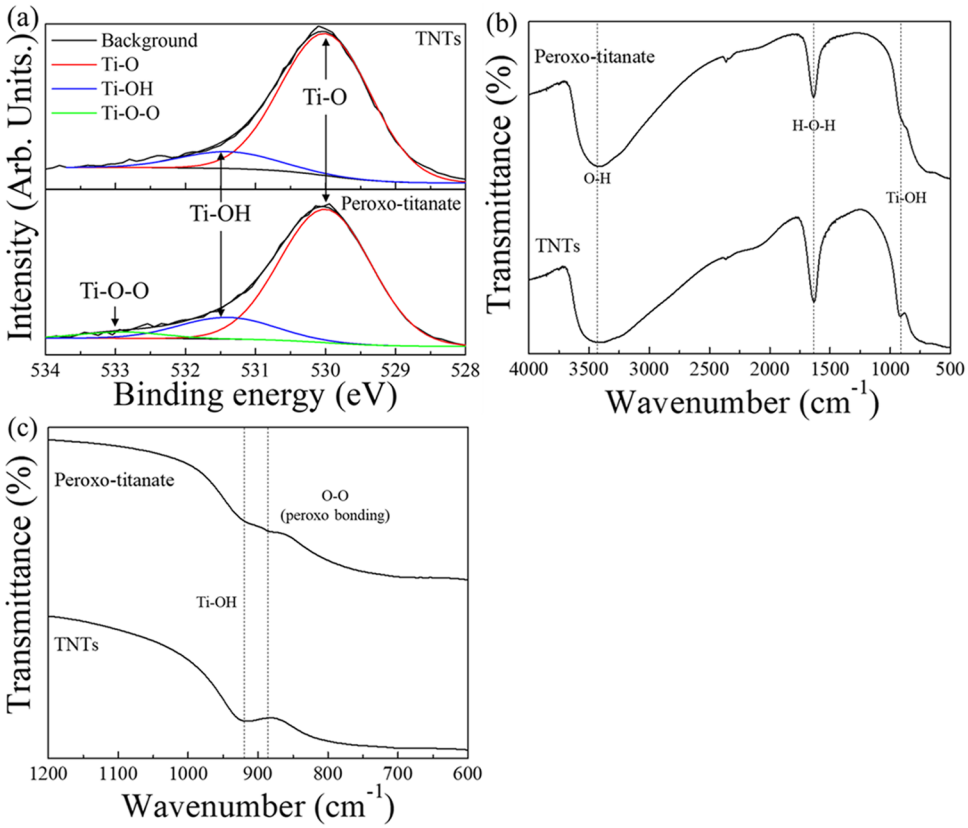

Figure 5. (a) XPS O 1s spectra of the peroxo-titanate and TNTs, (b) FT-IR spectra of the peroxo-titanate and TNTs, and (c) enlarged FT-IR spectra range of 1200−600 cm^{-1}.

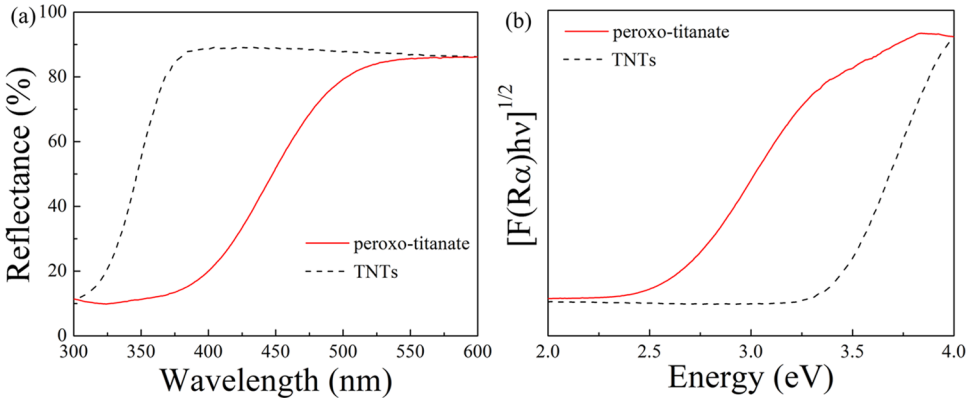

Figure 6. (a) UV−vis reflectance spectra and (b) Tauc plot graph of the peroxo-titanate and TNTs.

associated with the peroxo bonding (O−O). The layered titanate includes an OH bond at the end of the TiO_6 octahedron crystal in the interlayer.[35] The peroxo bond is expected to be combined with the titanium element in the final material to form Ti−O−O or Ti−O−O−H bonds. These results indicate that the existing Ti−OH bonding has been partially replaced by Ti−O−O bonding in the peroxo-titanate structure.

An interesting characteristic of peroxo-titanium bonding is that it causes a change in the energy band structure of titanate materials.[11] The peroxo-titanate sample has a yellowish color, unlike the conventional titanium oxide compound that is visually white and has a band gap of 3.2−3.4 eV, reflecting most of the light in the visible light region. In other words, peroxo-titanate absorbs a portion of visible light. Figure 6 shows the reflectance spectra and the Tauc plot of peroxo-titanate, which are compared to those of the conventional TNTs. As shown in Figure 6a, the peroxo-titanate sample has lower reflectance in the visible wavelength range than that of the pristine TNTs. This difference in optical properties results from the difference in the band gap between peroxo-titanate and TNTs. The Tauc plot used to investigate the band gap energy is presented in Figure 6b. The band gaps of the TNTs and peroxo-titanate were calculated based on the reflectance results using the Kubelka−Munk theory.[36]

As shown in Table 3, the TNTs and peroxo-titanate exhibit band gaps of 3.32 and 2.63 eV, respectively. The narrow band gap can extend the wavelength of light absorption, based on the formula $E = hc/\lambda$ (E is the photon energy, h is the Planck's constant, c is the speed of light, and λ is the wavelength of the

https://doi.org/10.1021/acsomega.4c05470
ACS Omega 2024, 9, 33293−33300

Table 3. Band Gap Energy of the Samples Calculated by the Kubelka Munk theory

Na:Ti (molar ratio)	band gap energy (eV)
peroxo-titanate	2.63
TNTs	3.32

photon).[37] When titanium is combined via peroxo bonding, the surrounding electron density of titanium is expected to decrease, causing an increase in the valence band of the semiconducting titanate materials.[11,38] Figure S2 shows the reflectance spectra and the Tauc plots of all titanate samples in the molar-ratio range of 10:1−1.1:1. These results also show that the peroxo-titanate samples synthesized by our method have similar levels of light absorption, regardless of the amount of TiH_2 used, which is similar to the tendency of the chemical compositions.

Figure 7 shows the FE-SEM (a−c) and STEM (d) images of peroxo-titanate observed at different magnifications. An anisotropic nanostructured aggregate with a width of 10−30 nm and high aspect ratio is identified. Although layered titanate possesses the characteristic of anisotropic crystal growth, the width of peroxo-titanate shows a partially irregular shape that is assumed to be due to partial scrolling effects similar to that in TNTs. Layered sodium titanate tends to form a nanosheet structure, which is estimated to change into a nanotube structure by ion exchange during the washing process.[39] Owing to the ion exchange phenomenon in which Na^+ is released, as the bonds between the Na^+ ions and TiO_6 layers disappear, the bonding force between the layers can be weakened and peeled off into a few layers. Furthermore, the exposed titanate layer can be scrolled to compensate for the increased surface energy.[8] This research also suggests that a scrolled nanosheet structure agglomerated by a similar formation mechanism has been formed. Figure S3 shows the SEM images of all titanate samples that are synthesized in a molar ratio of 10:1−1.1:1. The morphologies of the peroxo-titanates appear to exhibit a similar trend regardless of the molar ratio, and this similar morphology is attributed to the washing process, which results in all samples having the same chemical composition.

Figure 8 shows a schematic diagram of the results based on the amount of TiH_2 used. In this study, the relationship between the ionization energy of the mixed solution and the lattice energy of TiH_2 is studied. Although the 1:1 ratio is estimated to be ionizable, some TiH_2 remains after the reaction. In contrast, in the case of the molar-ratio range of 10:1−1.1:1, TiH_2 can be fully ionized to the PTC ion precursor, and layered sodium titanates are formed without impurities. The peroxo bonding in the PTC ions can be transferred from the synthesis process to the final product and can be present between layers or on the crystal surface. Based on these results, in this bottom−up method, it is concluded that the optimal amount of NaOH and TiH_2 for synthesis is possible with a maximum molar ratio of 1.1:1 (Na:Ti).

4. CONCLUSIONS

In this study, the optimal synthesis conditions for peroxo-bond-introduced layered titanate were explored by analyzing the ionization according to the amount of TiH_2 and the formation of the layered structure used in our bottom-up synthesis method. The results of the experiments and stoichiometric calculations showed that the ionization of TiH_2 was limited when the Na:Ti molar ratio was 1.1:1. The synthesized peroxo-titanate had a layered structure that allowed anisotropic growth to form a scrolled nanosheet structure with high aspect ratio. The amount of alkali raw material was reduced by 99.6 and 89.2% compared to that in the traditional hydrothermal method and the initial bottom-up process, respectively. The presence of peroxo bonds derived from the precursor in the interlayer and surface of the crystal structure caused band gap narrowing and extension of the absorbable light wavelength. This study presented an effective

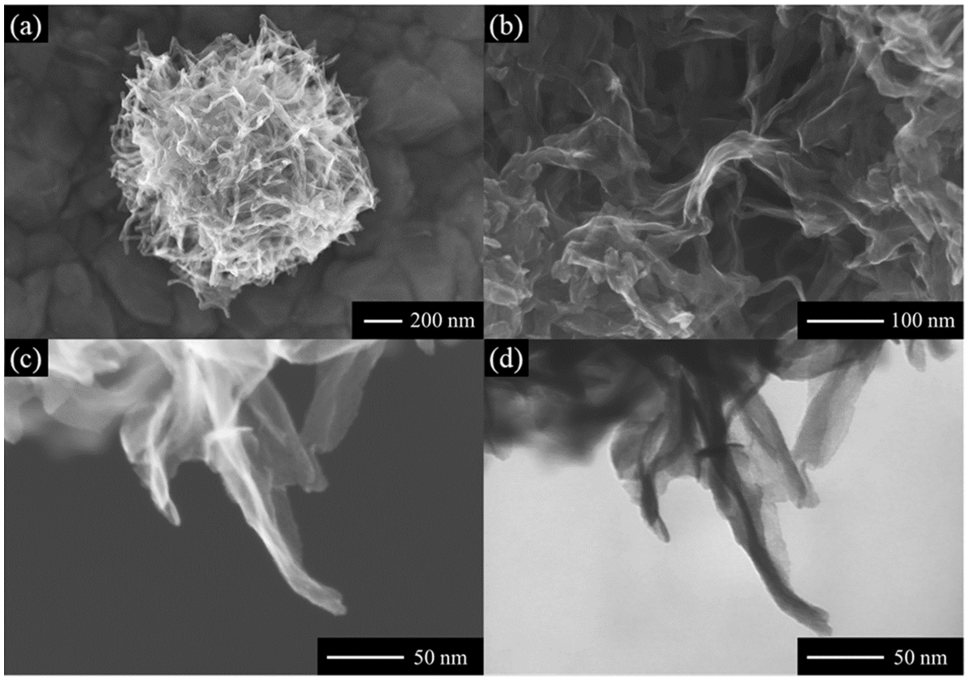

Figure 7. FE-SEM (a−c) and STEM (d) images of peroxo-titanate sample synthesized in Na:Ti molar ratio of 1.1:1.

https://doi.org/10.1021/acsomega.4c05470
ACS Omega 2024, 9, 33293−33300

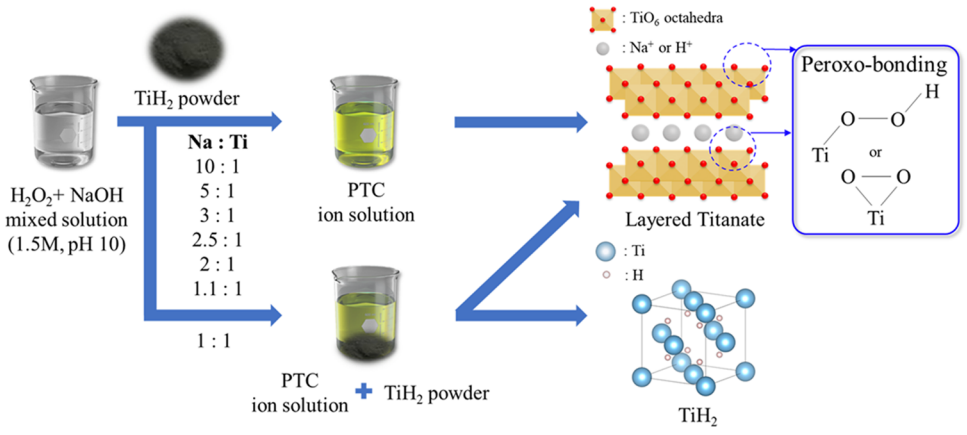

Figure 8. Schematic image of ionization and titanate synthesis according to the scale of TiH_2 (Na:Ti molar ratio).

method for synthesizing functionalized titanate nanostructures with low environmental impact and properties suitable for use in photochemistry-based applications.

■ ASSOCIATED CONTENT

Supporting Information

The Supporting Information is available free of charge at https://pubs.acs.org/doi/10.1021/acsomega.4c05470.

Experimental parameters and characterization of the synthesized products; amount of raw materials and products, and yield; XRD patterns of obtained product and reference material; optical properties (UV−vis reflectance spectra); SEM images showing morphologies of the products depending on the Na:Ti molar ratio in starting composition. (PDF)

■ AUTHOR INFORMATION

Corresponding Author

Tohru Sekino − *SANKEN (The Institute of Scientific and Industrial Research), Osaka University, Ibaraki, Osaka 567-0047, Japan;* orcid.org/0000-0002-6605-9166; Email: sekino@sanken.osaka-u.ac.jp

Authors

Do Hyung Han − *SANKEN (The Institute of Scientific and Industrial Research), Osaka University, Ibaraki, Osaka 567-0047, Japan;* orcid.org/0000-0001-5873-1728

Hyunsu Park − *SANKEN (The Institute of Scientific and Industrial Research), Osaka University, Ibaraki, Osaka 567-0047, Japan;* orcid.org/0000-0002-7239-3750

Tomoyo Goto − *SANKEN (The Institute of Scientific and Industrial Research), Osaka University, Ibaraki, Osaka 567-0047, Japan; Institute for Advanced Co-Creation Studies, Osaka University, Suita, Osaka 565-0871, Japan;* orcid.org/0000-0003-1362-6750

Yeongjun Seo − *SANKEN (The Institute of Scientific and Industrial Research), Osaka University, Ibaraki, Osaka 567-0047, Japan;* orcid.org/0009-0007-5668-5933

Yoshifumi Kondo − *SANKEN (The Institute of Scientific and Industrial Research), Osaka University, Ibaraki, Osaka 567-0047, Japan;* orcid.org/0000-0001-7189-2649

Sunghun Cho − *SANKEN (The Institute of Scientific and Industrial Research), Osaka University, Ibaraki, Osaka 567-0047, Japan;* orcid.org/0000-0002-6254-1094

Complete contact information is available at: https://pubs.acs.org/10.1021/acsomega.4c05470

Notes

The authors declare no competing financial interest.

■ ACKNOWLEDGMENTS

This research was supported by the Japan Science and Technology Agency (JST) under the Adaptable and Seamless Technology Transfer Program through Target-driven R&D (A-STEP) (JPMJTR22T8) and the "Dynamic Alliance for Open Innovation Bridging Human, Environment and Materials" in the "Network Joint Research Center for Materials and Devices" (MEXT, Japan). XRF and XPS analyses were performed at the Comprehensive Analysis Center, SANKEN, Osaka University, Japan.

■ ABBREVIATIONS

PTNT, peroxo-titanate nanotubes; PTC, peroxo-titanium complex; TNTs, titania nanotubes; XRD, X-ray diffraction; XRF, X-ray fluorescence; XPS, X-ray photoelectron spectroscopy; FTIR, Fourier transform infrared; UV−vis, ultraviolet−visible; FE-SEM, field-emission scanning electron microscopy; STEM, scanning transmission electron microscopy; FWHM, full width at half-maximum

■ REFERENCES

(1) Hu, W.; Li, L.; Li, G.; Liu, Y.; Withers, R. L. Atomic-Scale Control of TiO_6 Octahedra through Solution Chemistry towards Giant Dielectric Response. *Sci. Rep.* **2014**, *4*, No. 6582.

(2) Barim, G.; Dhall, R.; Arca, E.; Kuykendall, T. R.; Yin, W.; Takeuchi, K. J.; Takeuchi, E. S.; Marschilok, A. C.; Doeff, M. M. Heterostructured Lepidocrocite Titanate-Carbon Nanosheets for Electrochemical Applications. *ACS Appl. Nano Mater.* **2022**, *5*, 678−690.

(3) Cardoso, V. D. A.; Souza, A. G. D.; Sartoratto, P. P. C.; Nunes, L. M. The Ionic Exchange Process of Cobalt, Nickel and Copper(II) in Alkaline and Acid-Layered Titanates. *Colloids Surf., A* **2004**, *248*, 145−149.

(4) Saothayanun, T.; Sirinakorn, T. T.; Ogawa, M. Ion Exchange of Layered Alkali Titanates ($Na_2Ti_3O_7$, $K_2Ti_4O_9$, and Cs Ti_5O_{11}) with Alkali Halides by the Solid-State Reactions at Room Temperature. *Inorg. Chem.* **2020**, *59*, 4024−4029.

(5) Zhou, J.; Järvinen, T.; Pitkänen, O.; Kónya, Z.; Kukovecz, A.; Kordasb, K. Composites of Ion-in-Conjugation Polysquaraine and SWCNTs for the Detection of H_2S and NH_3 at ppb Concentrations. *Nanotechnology* **2021**, *32*, No. 185502, DOI: 10.1088/1361-6528/abdf06.

(6) Saothayanun, T. K.; Sirinakorn, T. T.; Ogawa, M. Layered Alkali Titanates ($A_2Ti_nO_{2n+1}$): Possible Uses for Energy/Environment Issues. *Front. Energy* **2021**, *15*, 631−655.
(7) Mao, Y.; Kanungo, M.; Benny, T. H.; Wong, S. S. Synthesis and Growth Mechanism of Titanate and Titania One-Dimensional Nanostructures Self-Assembled into Hollow Micrometer-Scale Spherical Aggregates. *J. Phys. Chem. B* **2006**, *110*, 702−710.
(8) Bavykin, D. V.; Parmon, V. N.; Lapkin, A. A.; Walsh, F. C. The Effect of Hydrothermal Conditions on the Mesoporous Structure of TiO_2 Nanotubes. *J. Mater. Chem.* **2004**, *14*, 3370−3377.
(9) Yu, J.; Yu, H. Facile Synthesis and Characterization of Novel Nanocomposites of Titanate Nanotubes and Rutile Nanocrystals. *Mater. Chem. Phys.* **2006**, *100*, 507−512.
(10) Rajeshwar, K.; Osugi, M. E.; Chanmanee, W.; Chenthamarakshan, C. R.; Zanoni, M. V. B.; Kajitvichyanukul, P.; Krishnan-Ayer, R. Heterogeneous Photocatalytic Treatment of Organic Dyes in Air and Aqueous Media. *J. Photochem. Photobiol. C* **2008**, *9*, 171−192.
(11) Park, H.; Goto, T.; Cho, S.; Nishida, H.; Sekino, T. Enhancing Visible Light Absorption of Yellow-Colored Peroxo-Titanate Nanotubes Prepared Using Peroxo Titanium Complex Ions. *ACS Omega* **2020**, *5*, 21753−21761.
(12) Kim, G.-S.; Seo, H.; Godble, V.; Kim, Y.; Yang, O.; Shin, H. Electrophoretic Deposition of Titanate Nanotubes from Commercial Titania Nanoparticles: Application to Dye-Sensitized Solar Cells. *Electrochem. Commun.* **2006**, *8*, 961−966.
(13) Townsend, T. K.; Browning, N.; Ostrerloh, F. E. Nanoscale Strontium Titanate Photocatalysts for Overall Water Splitting. *ACS Nano* **2012**, *6*, 7420−7426.
(14) Kasuga, T.; Hiramatsu, M.; Hoson, A.; Sekino, T.; Niihara, K. Formation of Titanium Oxide Nanotube. *Langmuir* **1998**, *14*, 3160−3163.
(15) Sreekantan, S.; Wei, L. C. Study on the Formation and Photocatalytic Activity of Titanate Nanotubes Synthesized via Hydrothermal Method. *J. Alloys. Compd.* **2010**, *490*, 436−442.
(16) Roux, H. l.; Glasser, L. Transferable Potentials for the Ti-O System. *J. Mater. Chem.* **1997**, *7*, 843−851.
(17) Liu, N.; Chen, X.; Zhang, J. A Review on TiO_2-Based Nanotubes Synthesized via Hydrothermal Method: Formation Mechanism, Structure Modification, and Photocatalytic Applications. *Catal. Today* **2014**, *225*, 34−51.
(18) Nakahira, A.; Kubo, T.; Numako, C. Formation Mechanism of TiO_2-Derived Titanate Nanotubes Prepared by the Hydrothermal Process. *Inorg. Chem.* **2010**, *49*, 5845−5852.
(19) Sallem, F.; Chassagnon, R.; Megriche, A.; el Maaoui, M.; Millot, N. Effect of Mechanical Stirring and Temperature on Dynamic Hydrothermal Synthesis of Titanate Nanotubes. *J. Alloys Compd.* **2017**, *722*, 785−796.
(20) Park, H.; Goto, T.; Han, D. H.; Cho, S.; Nishida, H.; Sekino, T. Low Alkali Bottom-Up Synthesis of Titanate Nanotubes Using a Peroxo Titanium Complex Ion Precursor for Photocatalysis. *ACS Appl. Nano Mater.* **2020**, *3*, 7795−7803.
(21) Park, H.; Goto, T.; Cho, S.; Lee, S. W.; Kakihana, M.; Sekino, T. Effects of Annealing Temperature on the Crystal Structure, Morphology, and Optical Properties of Peroxo-Titanate Nanotubes Prepared by Peroxo-Titanium Complex Ion. *Nanomaterials* **2020**, *10*, 1331.
(22) Luo, Y. R. *Comprehensive Handbook of Chemical Bond Energies*; CRC Press: Boca Raton, FL, 2007.
(23) Jenkins, H. D. B.; Morris, D. F. C. Philosophical Magazine Lattice Energies of Alkali Metal Nitrates and Related Thermodynamic Properties. *Philos. Mag.* **1977**, *35*, 1091−1097, DOI: 10.1080/14786437708232647.
(24) Brza, M. A.; Aziz, S. B.; Nofal, M. M.; Saeed, S. R.; Al-Zangana, S.; Karim, W. O.; Hussen, S. A.; Abdulwahid, R. T.; Kadir, M. F. Z. Drawbacks of Low Lattice Energy Ammonium Salts for Ion-Conducting Polymer Electrolyte Preparation: Structural, Morphological and Electrical Characteristics of CS:PEO:NH_4BF_4-Based Polymer Blend Electrolytes. *Polymers* **2020**, *12*, 1885.
(25) Lim, Y. W. L.; Tang, Y.; Cheng, Y. H.; Chen, Z. Morphology, Crystal Structure and Adsorption Performance of Hydrothermally Synthesized Titania and Titanate Nanostructures. *Nanoscale* **2010**, *2*, 2751−2757.
(26) Kapustinskii, A. F. Lattice Energy of Ionic Crystals. *Q. Rev. Chem. Soc.* **1956**, *10*, 283−294.
(27) Qamar, M.; Yoon, C. R.; Oh, H. J.; Lee, N. H.; Park, K.; Kim, D. H.; Lee, K. S.; Lee, W. J.; Kim, S. J. Preparation and Photocatalytic Activity of Nanotubes Obtained from Titanium Dioxide. *Catal. Today* **2008**, *131*, 3−14.
(28) Lan, Y.; Gao, X.; Zhu, H.; Zheng, Z.; Yan, T.; Wu, F.; Ringer, S. P.; Song, D. Titanate Nanotubes and Nanorods Prepared from Rutile Powder. *Adv. Funct. Mater.* **2005**, *15*, 1310−1318.
(29) Seo, H. K.; Kim, G. S.; Ansari, S. G.; Kim, Y. S.; Shin, H. S.; Shim, K. H.; Suh, E. K. A Study on the Structure/Phase Transformation of Titanate Nanotubes Synthesized at Various Hydrothermal Temperatures. *Sol. Energy Mater. Sol. Cells* **2008**, *92*, 1533−1539.
(30) Ylhäinen, E. K.; Nunes, M. R.; Silvestre, A. J.; Monteiro, O. C. Synthesis of Titanate Nanostructures Using Amorphous Precursor Material and Their Adsorption/Photocatalytic Properties. *J. Mater. Sci.* **2012**, *47*, 4305−4312.
(31) Bialik, M.; Sedin, P.; Theliander, H. Boiling Point Rise Calculations in Sodium Salt Solutions. *Ind. Eng. Chem. Res.* **2008**, *47* (4), 1283−1287.
(32) Qiu, Y.; Li, X. Synthesis of Peroxo-Titanium Decorated H-Titanate-Nanotube-Based Hierarchical Microspheres with Enhanced Visible-Light Photocatalytic Activity in Degradation of Rhodamine B. *Dalton Trans.* **2014**, *43*, 14537−14541.
(33) de Mendonça, V. R.; Lopes, O. F.; Avansi, W.; Arenal, R.; Ribeiro, C. Insights into Formation of Anatase TiO_2 Nanoparticles from Peroxo Titanium Complex Degradation under Microwave-Assisted Hydrothermal Treatment. *Ceram. Int.* **2019**, *45*, 22998−23006.
(34) Shin, S. S.; Yeom, E. J.; Yang, W. S.; Hur, S.; Kim, M. G.; Im, J.; Seo, J.; Noh, J. H.; Seok, S. I. Colloidally prepared La-doped $BaSnO_3$ electrodes for efficient, photostable perovskite solar cells. *Science* **2017**, *356*, 167−171, DOI: 10.1126/science.aam6620.
(35) Shirpour, M.; Cabana, J.; Doeff, M. New Materials Based on a Layered Sodium Titanate for Dual Electrochemical Na and Li Intercalation Systems. *Energy Environ. Sci.* **2013**, *6*, 2538−2547.
(36) Makuła, P.; Pacia, M.; Macyk, W. How To Correctly Determine the Band Gap Energy of Modified Semiconductor Photocatalysts Based on UV-Vis Spectra. *J. Phys. Chem. Lett.* **2018**, *9*, 6814−6817.
(37) Tan, L.-L.; Ong, W.-J.; Chai, S.-P.; Rahman Mohamed, A. Band Gap Engineered, Oxygen-Rich TiO_2 for Visible Light Induced Photocatalytic Reduction of CO_2. *Chem. Commun.* **2014**, *50*, 6923−6926.
(38) Etacheri, V.; Seery, M. K.; Hinder, S. J.; Pillai, S. C. Oxygen Rich Titania: A Dopant Free, High Temperature Stable, and Visible-light Active Anatase Photocatalyst. *Adv. Funct. Mater.* **2011**, *21*, 3744−3752.
(39) Ou, H. H.; Lo, S. L. Review of Titania Nanotubes Synthesized via the Hydrothermal Treatment: Fabrication, Modification, and Application. *Sep. Purif. Technol.* **2007**, *58*, 179−191.

https://doi.org/10.1021/acsomega.4c05470
ACS Omega 2024, 9, 33293−33300